All-Optical RZ-to-NRZ Conversion of Advanced Modulated Signals

Panos Groumas, Vasilis Katopodis, Christos Kouloumentas, Marios Bougioukos, and Hercules Avramopoulos

***Abstract*— A generic scheme for return-to-zero (RZ) to nonreturn-to-zero (NRZ) format conversion of optical signals is analyzed. It relies on a simple delay interferometer with frequency periodicity twice as high as the input symbol rate and a subsequent optical band-pass filter. Simulation results at 40 Gbaud indicate the compatibility of the technique with a variety of advanced modulation formats. RZ-to-NRZ conversion of 40 Gb/s differential phase shift keying signals is experimentally demonstrated with 1.5 dB power penalty compared to the back-to-back measurement.**

***Index Terms*— Format conversion, higher order modulation formats, integrated optics, phase modulation.**

I. Introduction

HIGH capacity, low cost and energy efficient interconnection between discrete optical network segments will depend on the availability of photonic subsystems capable of modulation format adaptation at the respective interfaces. Conversion from return-to-zero (RZ) to non return-to-zero (NRZ) format is a prominent example of the need for this type of subsystems at points where optical time-division-multiplexing (OTDM) are interfaced with wavelength-division-multiplexing (WDM) technologies.

Significant efforts have been made for RZ-to-NRZ conversion schemes relying either on Kerr-based nonlinearities [1]–[2], active elements [3]–[4], or linear configurations [5]–[8]. All these have been designed and investigated, however, only with conventional RZ on-off keying (RZ-OOK) or carrier suppressed RZ-OOK signals, despite that phase or generally advanced modulation formats are expected to dominate in next generation optical networks. Due to their simplicity and suitability for high speed operation, the linear configurations are particularly attractive for extending their operation with formats other than OOK. They rely on the use of a periodic filter with free-spectral range (FSR) twice as high as the line-rate and a subsequent optical band-pass filter (OBPF), and so far they have been used for RZ-OOK to NRZ-OOK conversion at 20 Gb/s using a simple delay interferometer (DI) [5] or up to 50 Gb/s using micro-resonators as periodic filters [6]–[7].

Manuscript received August 11, 2011; revised October 7, 2011; accepted October 28, 2011. Date of publication November 3, 2011; date of current version January 13, 2012. This work was supported in part by the European Union projects POLYSYS under Contract 258846 and APACHE under Contract 224326.

The authors are with the Photonic Communications Research Laboratory, National Technical University of Athens, Athens 15773, Greece (e-mail: pgrou@mail.ntua.gr; vkat@mail.ntua.gr; ckou@mail.ntua.gr; mpougiou@mail.ntua.gr; hav@mail.ntua.gr).

Color versions of one or more of the figures in this letter are available online at http://ieeexplore.ieee.org.

Digital Object Identifier 10.1109/LPT.2011.2174783

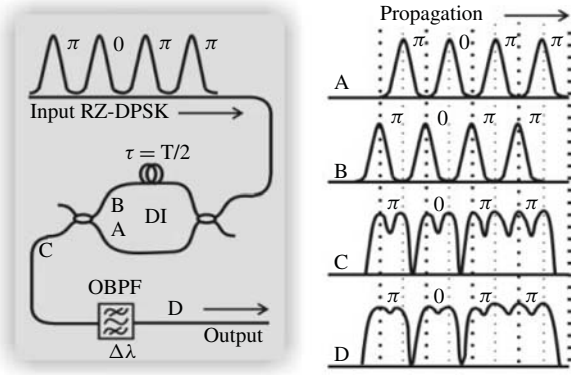

Fig. 1. Concept of RZ-to-NRZ conversion in the case of a DPSK signal.

In the present communication, we take the step further and investigate the compatibility of the DI-based conversion technique with advanced encoded signals. Simulations at 40 Gbaud reveal its potential for use with (differential) phase-shift keying ((D)PSK), (differential) quadrature phase-shift keying ((D)QPSK) and 16-quadrature amplitude modulation (16-QAM) signals. Experimental results at 40 Gb/s confirm that the phase information is not affected by the conversion mechanism, and demonstrate for the first time to our knowledge RZ-DPSK to NRZ-DPSK conversion with 1.5 dB power penalty compared to the back-to-back case.

II. Concept and Simulation Study

Fig. 1 describes the operating principle of the converter for an input RZ-DPSK signal. Depending on the data sequence, the RZ pulses present an additional 0 or π rad phase. The DI exhibits a time delay τ that is equal to half the symbol period T. In this way, the DI replicates the input signal and adds in-phase at point C the original pulses arriving from the lower arm (point A) with their delayed replicas arriving from the upper one (point B). The common stream is then driven through the OBPF before getting to the final output of the circuit (point D). The right panel of Fig. 1 shows the relative timing at the different points, and provides an insight into the conversion mechanism. For the phase values of the pulses at point B, we have also taken into account the $\pi/2$ phase- shift that the pulses will experience through the second DI coupler towards the output port. For realistic values of the input duty-cycle, the original pulses and their replicas in the combined stream (point C) overlap in time, add in-phase and extend the duty-cycle such that the high-power level is sustained over the whole symbol period. In the case that successive symbols have

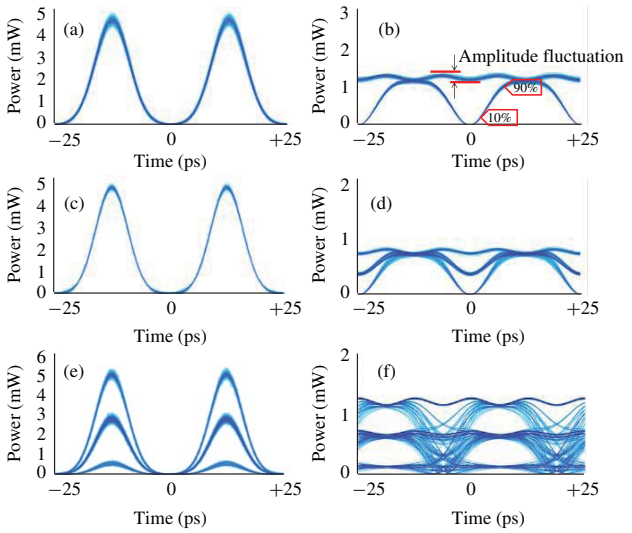

Fig. 2. Simulation results (eye-diagrams) for 40 Gbaud modulated signals (a)–(b) input RZ- and converted NRZ-DPSK signals, (c)–(d) input RZ- and converted NRZ-DQPSK signals, and (e)–(f) input RZ-and converted NRZ-16-QAM signals. The duty-cycle of all input signals is 33%.

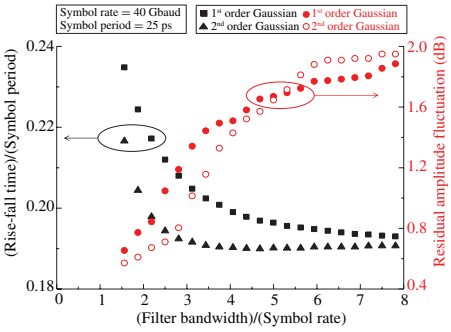

Fig. 3. Rise/fall times (10%–90%) of the intensity dips and residual amplitude fluctuation of the converted NRZ-DPSK signal as a function of the OBPF. Normalized values are used for the rise/fall times and the filter bandwidth.

the same phase, their overlapping pulses add also in-phase and sustain the high-power level beyond a single symbol. In the opposite case their combination is out-of-phase and results in the intensity dips of Fig. 1. The amplitude fluctuation at point C depends on the shape and the duty-cycle of the input pulses. It can be smoothed out with an OBPF (point D) at the expense of slower rise and fall times in the dips, and thus increased effect of the timing jitter due to the reduced time window around the center of each symbol. It is noted that the same result can be obtained also in the case that the OBPF precedes the DI due to the linear combination of the two filters.

Fig. 2 summarizes the main simulation results with DPSK signals and higher order modulation formats. Fig. 2(a) shows the input 40 Gb/s RZ-DPSK signal with Gaussian pulses and 33% duty-cycle. The resultant NRZ-DPSK signal after an 80 GHz DI and a 0.6 nm (75 GHz) OBPF is shown in Fig. 2(b), and it is in agreement with the analysis presented above. Fig. 2(c) and Fig. 2(d) present the respective simulated eye-diagrams for an input 40 Gbaud RZ-DQPSK signal with Gaussian pulses and 33% duty-cycle, too. The additional level in the intensity dips of the output eye-diagram corresponds to transitions between adjacent symbols with ±90° phase difference. Finally, Fig. 2(e) and 2(f) depict the respective

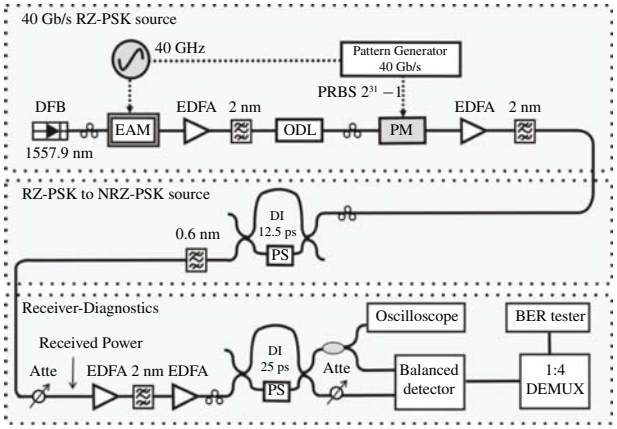

Fig. 4. Experimental setup for the RZ-to-NRZ conversion of DPSK signals.

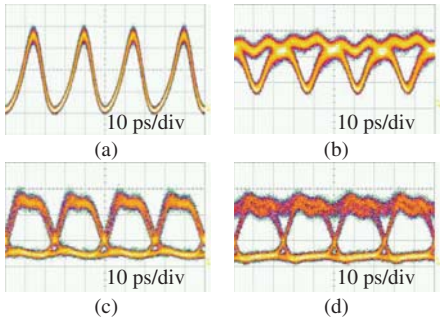

Fig. 5. Experimental results. Eye-diagrams of (a) input RZ-PSK signal, (b) converted NRZ-PSK signal, and (c)–(d) corresponding decoded streams.

eye-diagrams for a 40 Gbaud RZ-16-QAM signal with the same pulse shape and width as previously. Despite the additional levels in the dips due to the multitude of phase and amplitude combinations between successive symbols, the eye-diagram of the converted signal remains clearly open indicating the efficiency of the method.

Factors that may deteriorate the performance of the converter include the phase-shift difference between the arms of the DI, the time delay deviation in the DI and the frequency offset between the center of the OBPF pass-band and the input signal. The phase-shift difference prevents the in-phase addition of the pulses at the DI output and results in enhanced amplitude fluctuation and reduced output power. Nevertheless, phase-shift differences within the ±40° range are expected to be sufficiently tolerated by the format converter. Time delays between the DI arms that are not equal to half the symbol rate also result in higher amplitude fluctuations in the converted signal. In this case, deviations within the ±10% range around the ideal delay are still tolerable. Finally, the frequency offset between the OBPF pass-band and the input signal deteriorates the performance of the converter in a way similar to the way the phase-shift deviation in the DI also does. The impact of the offset, though, remains low for all considered formats (DPSK, DQPSK and 16-QAM) even for offsets in excess of 50% of the symbol-rate. As such, the relevant impact is expected to be quite limited in practical implementations of the technique.

Fig. 3 refers back to the 40 Gb/s DPSK case commenting on the dependence of the 10-to-90% transition times in the dips and the dependence of the residual fluctuation on the

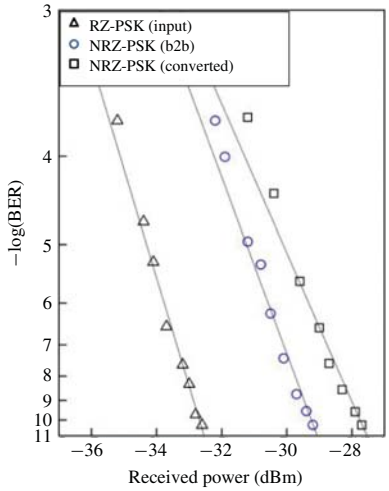

Fig. 6. BER curves for the input RZ-PSK, the converted NRZ-PSK, and the back-to-back (b2b) NRZ-PSK signal.

OBPF. The two metrics are defined in Fig. 2(b). As the filter determines the bandwidth of the converter, it results in a basic trade-off between the dip duration and the fluctuation at the high power level. This is aligned with previous studies on OOK signals [7]. In Fig. 3 the rise/fall times and the filter bandwidth are normalized in order to allow direct scaling to other line rates.

III. Experimental Setup and Results

The experimental investigation of the technique with 40 Gb/s PSK signals was based on the setup of Fig. 4. The output of the distributed feedback (DFB) laser at 1557.9 nm was inserted into the electro-absorption modulator (EAM) for pulse carving at 40 GHz. The optical clock with 8.5 ps pulse width (∼33% duty-cycle) was amplified by an erbium-doped fiber amplifier (EDFA) and forwarded through an optical delay line (ODL) to the phase modulator (PM) that was driven by the $2^{31}-1$ long pseudo-random bit sequence (PRBS). The 40 Gb/s output RZ-PSK signal entered the format conversion stage consisting of an integrated 80 GHz DI and a 0.6 nm OBPF. The polarization controller at the input of the DI was required in order to adjust the polarization of the input signal due to the material birefringence in the silica-on-silicon motherboard of the DI, and thus the polarization sensitivity of the integrated device. Correct phase addition of successive bits was ensured by a thermo-optic phase shifter (PS) in the lower arm of the DI. The insertion loss of the whole format converter was 12.5 dB, mainly due to the 11 dB insertion loss of the integrated DI. After conversion, the NRZ-PSK signal was forwarded to the receiver unit. The attenuator (atte) adjusted the power and thus the optical signal-to-noise ratio (OSNR) of the received signal. After pre-amplification and amplification, the signal entered the 40 GHz DI for decoding, and the two complementary OOK streams were driven to the balanced detector with −1 dBm power. Finally, the electrical signal was 1 : 4 demultiplexed and evaluated through bit-error rate (BER) measurements. The eye-diagrams of the phase-encoded and the decoded signals were visualized by a single-ended photoreceiver.

Fig. 5 summarizes the main results. Fig. 5(a) and 5(b) depict the input RZ-PSK and the converted NRZ-PSK signal. Fig. 5(c) and 5(d) present in turn the alternate-mark inversion (AMI) and duobinary (DB) streams at the outputs of the 40 GHz DI after decoding of the converted signal. Both eye-diagrams are clearly open indicating the high quality of the NRZ-PSK signal and the overall efficiency of the technique. Finally, Fig. 6 presents the BER curves for the input RZ-PSK, the converted NRZ-PSK and the back-to-back (b2b) NRZ-PSK signal. Each curve corresponds to the worst among the four 10 Gb/s tributaries of each signal. The variation among the four tributaries was negligible though due to the passive nature of the technique, and thus the absence of any patterning effects. Error free format conversion was confirmed with less than 5 dB power penalty compared to the input RZ-PSK signal. It is noted that this penalty was mainly due to the different average over peak power ratios that correspond to the two formats. The respective power penalty of the converted signal compared to the b2b NRZ-PSK stream was less than 1.5 dB indicating the limited degree of distortion induced by the conversion mechanism. For this comparison, we assumed as b2b, the 40 Gb/s signal at the output of the same phase modulator, when the latter was operated with a continuous wave (cw) optical input again at 1557.9 nm. We expect that the 1.5 dB power penalty can be even lower if the duty-cycle of the input RZ-PSK stream is greater than 33%. This is supported by the findings of previous relevant studies in the case of RZ-OOK to NRZ-OOK format conversion using the same technique [5].

IV. Conclusion

We have experimentally demonstrated RZ-to-NRZ conversion of 40 Gb/s DPSK signals with 1.5 dB power penalty using a periodic filter (DI) and an OBPF. Simulations at 40 Gbaud with DPSK, DQPSK and 16-QAM signals have indicated the compatibility of the technique with higher-order modulation formats and, thus, its potential for use in multi-format processing network nodes.

References

[1] S. Bigo, E. Desurvire, and B. Dersuelle, "All-optical RZ-to-NRZ format conversion at 10 Gbit/s with nonlinear optical loop mirror," *Electron. Lett.*, vol. 30, no. 22, pp. 1868–1869, Oct. 15, 1994.

[2] S. H. Lee, K. K. Chow, and C. Shu, "Spectral filtering from a cross-phase modulated signal for RZ to NRZ format and wavelength conversion," *Opt. Express*, vol. 13, no. 5, pp. 1710–1715, 2005.

[3] X. Lei, B. C. Wang, V. Baby, I. Glesk, and P. R. Prucnal, "All-optical data format conversion between RZ and NRZ based on a Mach-Zehnder interferometric wavelength converter," *IEEE Photon. Technol. Lett.*, vol. 15, no. 2, pp. 308–310, Feb. 2003.

[4] C. W. Chow, C. S. Wong, and H. K. Tsang, "All-optical RZ to NRZ data format and wavelength conversion using an injection locked laser," *Opt. Commun.*, vol. 223, nos. 4–6, pp. 309–313, Aug. 2003.

[5] X. Zhang, Y. Yu, H. Dexiu, L. Lijun, and F. Wei, "20-Gb/s all-optical format conversions from RZ signals with different duty cycles to NRZ signals," *IEEE Photon. Technol. Lett.*, vol. 19, no. 14, pp. 1027–1029, Jul. 15, 2007.

[6] Y. Zhang, E. Xu, D. Huang, and X. Zhang, "All-optical format conversion from RZ to NRZ utilizing microfiber resonator," *IEEE Photon. Technol. Lett.*, vol. 21, no. 17, pp. 1202–1204. Sep. 1, 2009.

[7] Y. Ding, *et al.*, "Multi-channel WDM RZ-to-NRZ format conversion at 50 Gbit/s based on single silicon microring resonator," *Opt. Express*, vol. 18, no. 20, pp. 21122–21130, 2010.

[8] Y. Yu, X. Zhang, and D. Huang, "All-optical format conversion from CS-RZ to NRZ at 40 Gbit/s," *Opt. Express*, vol. 15, no. 9, pp. 5693–5698, 2007.